


Magnetic and spectrometric studies of Al-Gor area, Southwestern Sinai, Egypt

Mostafa A. M. ZAEIMAH 

Nuclear Materials Authority

P. O. Box 530 Maadi, Cairo, Egypt

e-mail: mostafazaeima@yahoo.com, mostafazaeima@gmail.com

Abstract: Al-Gor area is a part of Southwestern Sinai of Egypt. It is considered as one of the most promising areas for mineralization in Egypt, being rich in many mineral deposits of: manganese, iron, copper, zinc, lead, cobalt, nickel, silver, gibbsite, and uranium. Besides, some industrial ore minerals such as kaolin and glass sand, . . . etc. are also found in this area. The area was studied by Gama-ray spectrometry to trace the radioactive anomalies, their concentrations and their relationship to the existing rocks, and by magnetic survey to study the relationship of radioactive anomalies and their trends with the trends of geological structures. The gamma-ray spectrometric maps show different levels over the surveyed area, which reflect contrasting radioelement contents for the exposed various rock types. The highest radiospectrometric levels are located in the northwest southeast direction and some scattered parts all over the study area. They are mainly associated with Um-Bogma Formation, bearing gibbsite. The study area possesses radiospectrometric ranging between 0.6 and 110.9Ur as a total-count, 0.1 to 1.8% for K, 0.1 to 99 ppm for eU and 0.1 to 23 ppm for eTh. The qualitative analyses of magnetic data show the existences of a number of different magnetic anomalies, with different amplitudes and frequencies as well as trends. From the application of spectral analyses of magnetic data, the regional and residual depths of magnetic anomalies can be computed. The first depth represents the regional (deep-seated) anomalies, at about 75 m and the residual (shallow-seated) anomalies, at about 20 m. The trends of the structures as derived from the spectrometric and ratio maps correspond to those inferred from the residual-component magnetic map, which reflects the effect of structures on the concentration of radioactive elements and, consequently mineralization.

Key words: gamma-ray spectrometry, ground magnetics, regional and residual depths of magnetic anomalies, gibbsite, Al-Gor area, Sinai

1. Introduction

The southwestern part of Sinai is considered as one of the most promising areas for heavy metal mineralization in Egypt, being rich in many mineral deposits besides, some industrial ore minerals.

Al-Gor area is a part of the Southwestern Sinai of Egypt. It is occupied by Paleozoic rocks. The Paleozoic succession (of 160–370 m in thickness) is subdivided into seven formations, which are (from the oldest) Sarabit El-Khadim, Abu-Hamata, Adediya, Um-Bogma, El-Hashash, Magharet El-Maiah and Abu-Zarab (*Soliman and Abu El-Fetouh, 1969* and *Alshami, 2003*). The study area was subjected to intensive geological and geochemical studies, which revealed that a possible gibbsite, and uranium, are related to Um-Bogma Formation. Ground geophysical follow-up surveys were applied on this area.

2. Aim of geophysical study

An airborne geophysical survey for Southwestern Sinai was carried out by Nuclear Materials Authority (NMA) of Egypt in 1998. They involved magnetic and gamma-ray spectrometric surveys, which led to the discovery of some important occurrences of radioactive mineralization. The processing of these data identified many zones, which needed further verification and ground geophysical follow-up. Accordingly, Al-Gor area was selected as a hopeful target for uranium potentiality. Hence, ground geophysical survey was applied to this area. The area was studied by Gamma-ray spectrometry to trace the radioactive anomalies, their concentrations and their relationship to the existing rocks. The aim of the magnetic study is to define the most significant magnetic anomalies, which may be related to surface and/or subsurface anomalies and to delineate the structural setting, which may control the distribution of the mineralization in the study area. The present study deals with the use and correlation between the obtained data and the geology of the study area to infer the relation, which might exist between the mapped surface geologic structures and the interpreted subsurface structures.

3. Geological outlines

The study area is surrounded by rock exposures ranging from Precambrian to Quaternary (Fig. 1). The Precambrian comprises granodiorites and granites. The Paleozoic rocks comprise seven formations, from base to top: Sarabit El-Khadim, Abu-Hamata, Adediya, Um-Bogma, El-Hashash,

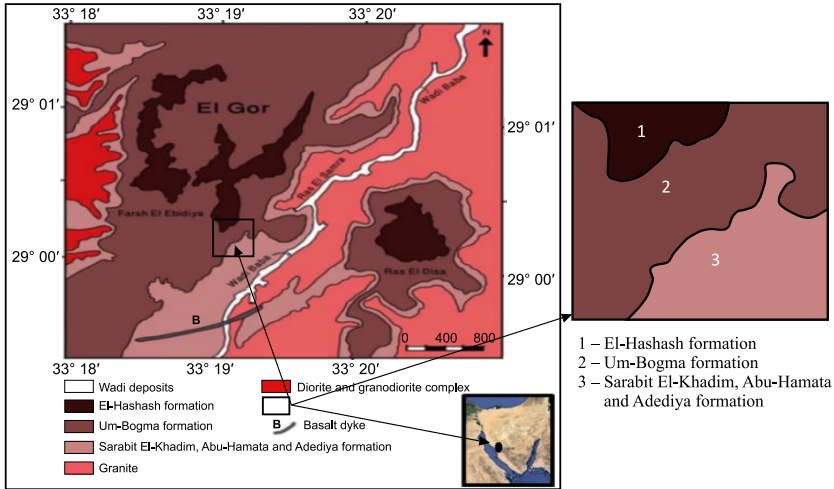


Fig. 1. Geologic map of El-Gor area, Southwestern Sinai, Egypt (Attia et al., 2011).

Magharet El-Maiah and Abu-Zarab. Magharet El-Maiah and Abu-Zarab formations are not located in the study area.

- El-Hashash Formation: It consists of brownish, cross laminated sandstones, intercalated with thin shale and siltstone beds.
- Um-Bogma Formation: This formation can be regarded as a poly-mineralized rock unit including (U, Th, Cu, and REEs,) (Alshami, 2018 and Alkhateeb et al., 2019). It can be classified into three members:
 - Upper dolostone: It is mainly composed of pinkish brown, hard and compact crystalline-bedded dolostone.
 - Middle marl and dolostone: It is a yellow bed that consists mainly of marl and dolostone, with some intercalated shales. Gypsum, anhydrite and halite are also found.
 - Lower siltstone, dolostone, claystone: The dolostone is compact, fractured and jointed with patches of different green colours. Besides, the ferruginous siltstone is large and extends at most parts of the study area.
- Adediya Formation: The lower contact of Adediya Formation is well defined, but the upper one is highly ferruginated and in some parts shows

signs of paleosoil. It consists of sandstone, very thickly-bedded, fine-grained, yellow, red and white in colour.

- Abu-Hamata Formation: It is easily distinguished by its characteristic greenish colour, which can be used as a marker in the field.
- Sarabit El-khadim Formation: The lower boundary of this formation is represented by a nonconformity with the underlying basement rocks. Cross-bedded sandstone with a conglomerate layer alternating with the sandstone in most localities (*Soliman and Abu El-Fetouh, 1969*).

4. Ground gamma-ray spectrometric survey

Gamma-ray methods (*Durrance, 1986*) use scintillometer to identify the presence of the natural radioelements: potassium, uranium, and thorium. Multi-channel spectrometers can provide measures of individual radioelement abundances. Gamma-ray methods have had wide applications in uranium exploration because they provide direct detection. Thorium is generally the most immobile of the three radioelements and has geochemical behaviour similar to that of zirconium. Thorium content, like uranium content, tends to increase in felsic rocks and generally increases with alkalinity.

Spectral gamma-ray measurements were conducted for the study area along a number of profiles directed N–S. The spacing between these profiles were 50 m, while the interval between stations were 20 m, using a portable gamma-ray spectrometer; model GS-512, manufactured by Geofyzika Brno (*Geofyzika, 1997*), Czech Republic. The spectrometer was calibrated using the locally constructed Nuclear Materials Authority of Egypt transportable concrete calibration pads.

4.1. Qualitative interpretation

Qualitative interpretation of the ground gamma-ray spectrometric data depends mainly upon the excellent correlation between the general pattern of recorded measurements and the surface distribution of rock units. The texture of the radio-spectrometric contour lines (signatures) could be an aid in the course of interpretation of surface geology (lithology and structure) (*IAEA, 1979*).

The study area is mainly covered by Um-Bogma Formation (2), (Fig. 1) and Sarabit El-Khadim, Abu-Hamata, and Adediya formations (3) in the southern part of the study area, with small parts covered with El-Hashash Formation (1) in the northern part (Fig. 1). Gamma-ray spectrometric maps (Fig. 2) show various levels with different colour over the surveyed area. These levels reflect contrasting radioelement contents for the exposed various rock types. From the four maps (Fig. 2) of the total count (T.C.), potassium (K), equivalent uranium (eU) and equivalent thorium (eTh), a number of radiospectrometric anomalies with different shapes and sizes are

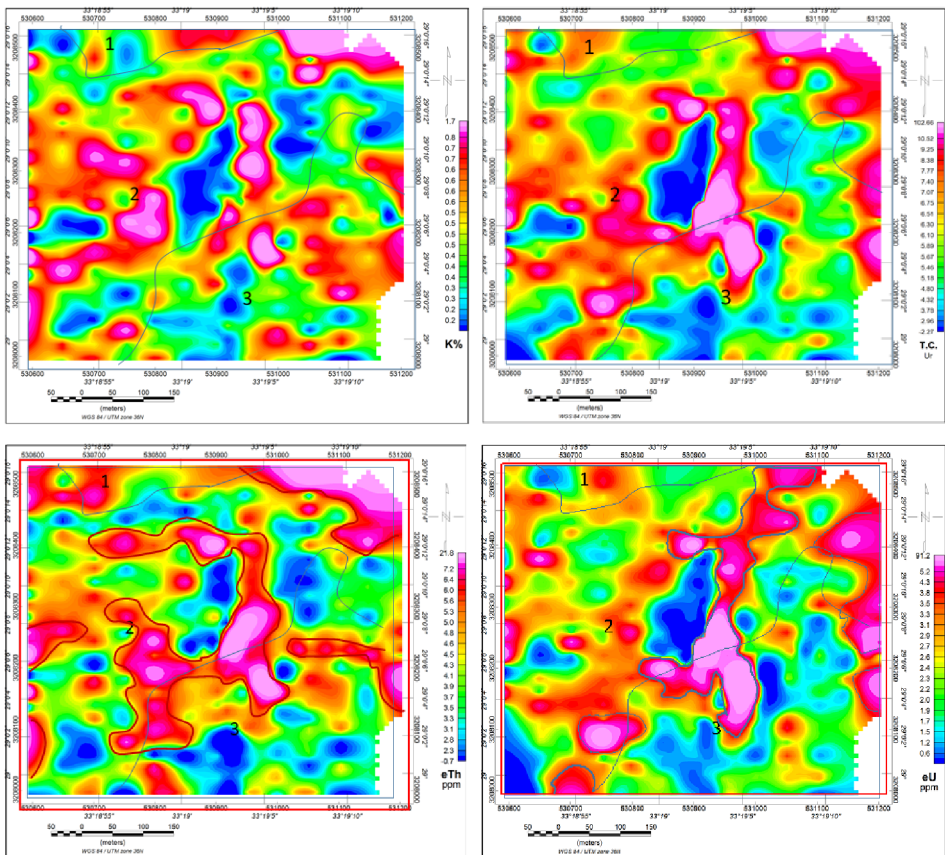


Fig. 2. Filled colour contour map of Total Count (T.C.), K, eU and eTh data, Al-Gor area, southwestern Sinai, Egypt.

dispersed in the study area in all directions: north, south, east and west. There are some anomalies on the four maps that take a northeast-southwest trend, at the contact between Um-Bogma formation and Sarabit El-Khadim, Abu-Hamata, and Adediya formations as well as in the far northeast. Most of the highest value anomalies are associated with the presence of gibbsite, which is found in some locations of the study area. There is an agreement to a large extent in the locations and shapes of the radiometric anomalies on the four maps. The thickly marked polygons in the eU map (Fig. 2) represent U concentrations in the range 4–20 ppm, while in the eTh map represent eTh concentrations in the 5–40 ppm range. In eTh/eU map (Fig. 3), the thickly marked polygons represent $eTh/eU < 1$, while, the polygons in eU/K map represent $eU/K > 5-10$.

4.2. Quantitative interpretation

El-Hashash formation (1) (Fig. 1) is characterized by low to intermediate concentrations in T.C.,K, eU and eTh, ranging from 1 to 7 Ur, 0.1 to 0.7%, 1 to 4 ppm and 1 to 7 ppm, respectively. Meanwhile the other two (2,3 formations) are characterized by concentrations varying from low to very high in the four variables. Table 1 shows the statistical values of the radiometric data for the study area.

Table 1. Computed statistical characteristics of radiometric data of Al-Gor area, southwestern Sinai, Egypt.

Variable	Min.	Max.	X	S
T.C. (Ur)	0.6	110.9	7.5	9.4
K%	0.1	1.8	0.5	0.3
eU (ppm)	0.1	99.1	3.7	8.2
eTh (ppm)	0.1	23.0	4.7	2.7
eU/eTh	0.03	5.3	0.74	0.63
eU/K	0.25	330.33	8.78	20.06
eTh/K	1.0	76.67	11.28	8.19
X = mean				
S = standard deviation				

The character of radiometric anomalies, associated with subsurface and outcropping U mineralization, depends on the forms of U mineralization,

the host rock, and the geological setting. Typical features of U mineralization, detected at the earth’s surface are (Krasnov *et al.*, 1980):

1. Elliptical dispersion halos with dimensions from 70×80 m up to 80×350 m,
2. Anomalous U concentrations in the range of 4–20 ppm eU,
3. Associated Th anomalies in the range of 5–40 ppm eTh,
4. Ratios between the radioelement of $Th/U < 1$, $U/K > 5-10$, Th/K in the range 4–5, and
5. Increasing gamma radiation with depth.

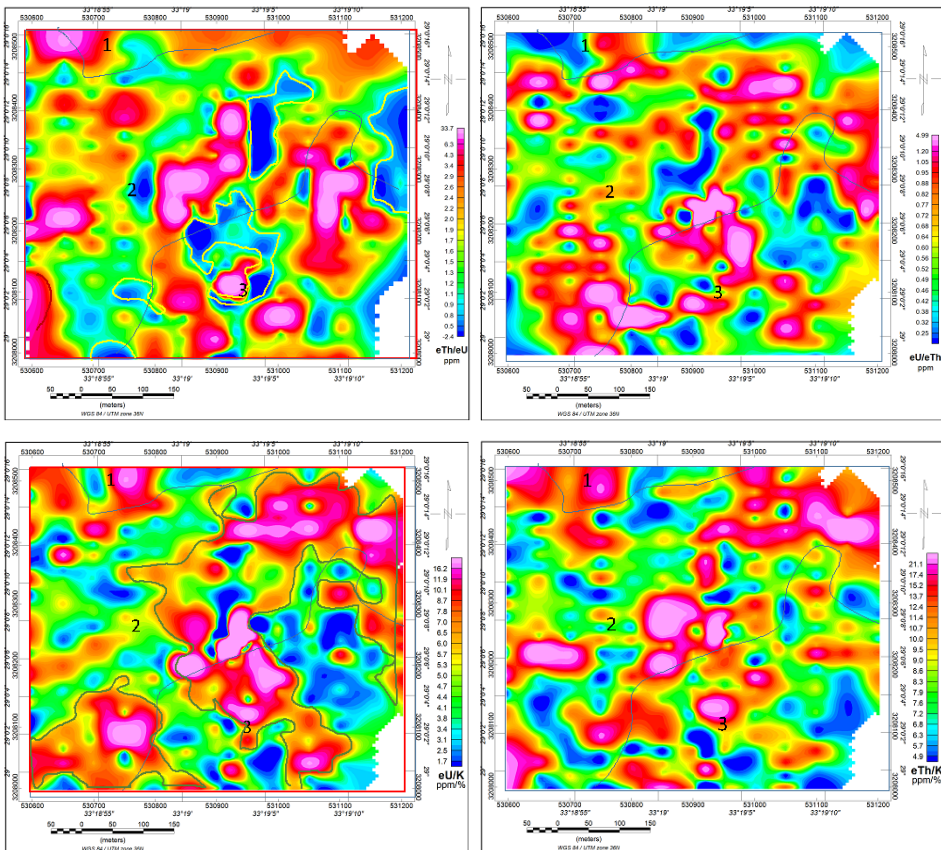


Fig. 3. Filled colour contour maps of eU/eTh, eU/K, eTh/K and eTh/eU data, Al-Gor area, southwestern Sinai, Egypt.

When applying these five requirements of (*Krasnov et al., 1980*) to the studied area, and from examination of the four ratio maps eU/eTh, eU/K, eTh/eU, and eTh/K (Fig. 3), it can be noticed that there is more than one site, in which these specifications are available to give a good impression to the possibility that they are suitable for uranium exploration (Fig. 4). Accordingly, other steps can be started, such as trenching and drilling to track radioactive anomalies at different depths. Consequently, it is recommended to use other geophysical methods, such as the electrical method, to trace and follow gibbsite at depth, as it is correlated with high concentrations of uranium.

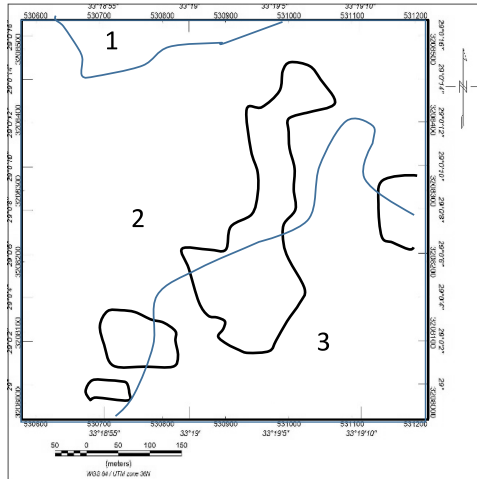


Fig. 4. Interpreted anomalies as deduced from *Krasnov et al. (1980)* of eU, eTh, eTh/eU, eU/K and eTh/K data, Al-Gor area, southwestern Sinai, Egypt.

4.3. Outlining uranium anomalous zones

Combination of two or more data sets into a single display creates composite colour images. Such images facilitate the spatial correlation of features in various input data sets (*Broome, 1990*). Examination of the high zones of eU, eU/eTh and eU/K can help in defining uranium enrichment over the other two natural radioelements (Th and K). As for economic potential, the most promising uranium anomalies should have a high eU abundance coinciding with high eU/eTh and eU/K ratios (*Saunders and Potts, 1976*).

Accordingly, a uranium composite image map (Fig. 5a) was produced to identify and outline the most probable uranium anomalous zones. So, the eU composite image map (Fig. 5a) can provide useful information regarding the identification of anomalous zones of enriched uranium concentration. This map combines eU (in blue) with the two ratios eU/K (in red) and eU/eTh (in green). The uranium anomalous zones are displayed as white portions on both the uranium and radioelement composite image maps. These uranium-enriched zones offer good prospects for uranium, since their relatively high concentrations of uranium with respect to both potassium and thorium are important diagnostic factors in the recognition of possible uranium deposits (IAEA, 1988). Examination of Figures 4 and 5 indicates a fair good agreement in the sites with high concentrations of uranium, which gives great confidence in the results obtained from the two methods of *Krasnov et al. (1980)* and *Broome (1990)* used to determine the high ranges of uranium concentrations, which may raise the probability to consider the study area as a new site for uranium exploration. The radiometric studies on soil sediments in and around the investigated area, reflects an increase of uranium concentration with depth. Almost all of the studied rock types gave from chemical analyses a greater amount of uranium than those determined

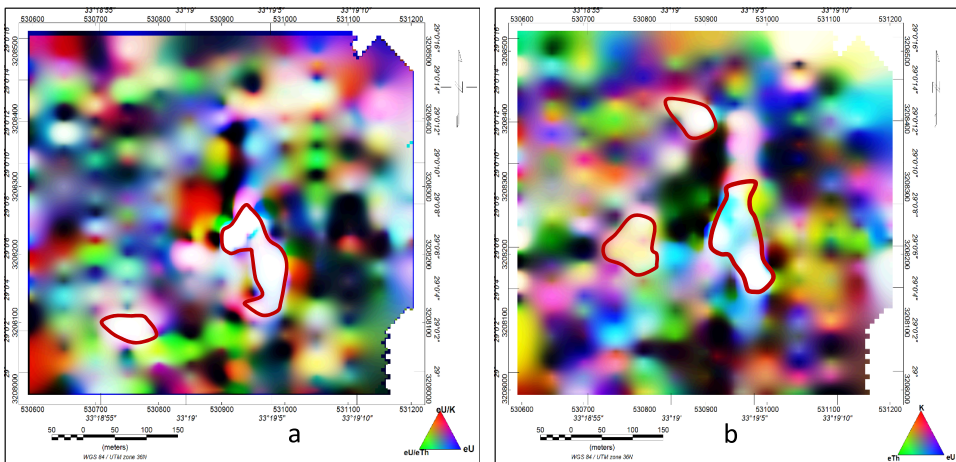


Fig. 5. Projection of the interpreted anomalous zones as deduced from Uranium Composite image (a) and radioelement composite image (b) maps of Al-Gor area, south western Sinai, Egypt.

radiometrically, reflecting a disequilibrium state, characterizing by addition of uranium (*Abdel-Azeem, 2011*).

5. Ground magnetic survey

The ground magnetic survey was conducted along numerous profiles in the study area directed N–S. The spacing between these profiles was 50 m, while the interval between stations was 20 m. These profiles cut across most of the surface mineralization of and structural features, which were recorded in the study area. As a result of this survey, a total magnetic intensity (TMI) contour map (Fig. 6) was constructed and interpreted to obtain subsurface information about the extensions and depths of the recorded magnetic anomalies, which may represent an insight to the subsurface distribution of radiospectrometric anomalous zones beneath ground surface.

The ground magnetic survey was conducted along the study area using two proton precession magnetometers; model PMg-1, one for recording

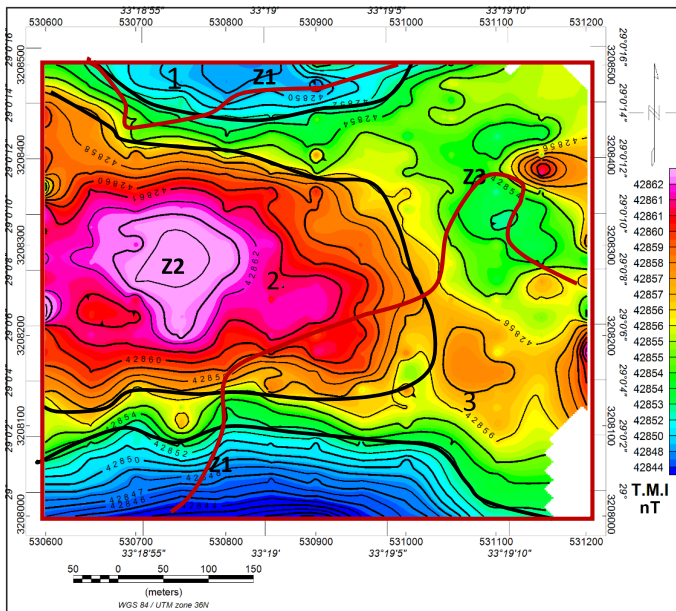


Fig. 6. Filled-colour contour map of the total magnetic intensity (TMI) data, Al-Gor area, Southwestern Sinai, Egypt.

variations of the total magnetic intensity field, and the other for recording its diurnal variations in a selected base station, sited near the study area. These two instruments are sensitive to any changes of the total magnetic field intensity of the earth’s magnetic field and their accuracy reach about 0.01 nT. Accordingly, the corrected ground magnetic field intensity measurements at the study area were plotted in the form of a contour map (Fig 6).

5.1. Qualitative interpretation

The ground total-intensity magnetic field recorded over the area under study represents the combined contribution of surface magnetic sources and deep-seated sources. Close investigation of the total-intensity magnetic map (Fig. 6) shows a number of different magnetic anomalies, with different amplitudes and frequencies. The variations in amplitudes of these magnetic anomalies may reflect changes in the composition of the rocks. Meanwhile,

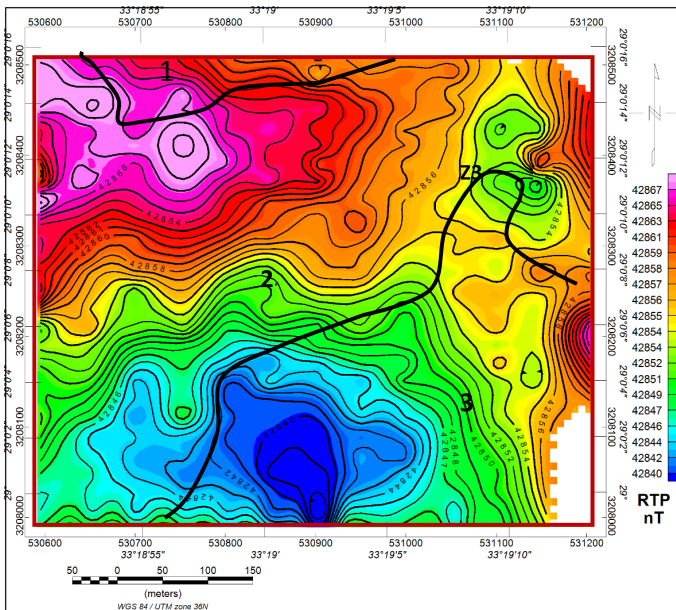


Fig. 7. The reduced to the north magnetic pole (RTP) map, Al-Gor area, Southwestern Sinai, Egypt.

the variations in wavelengths of the mentioned magnetic anomalies may indicate variations in the depths of their causative bodies. The study area can be divided into three different magnetic zones (Z1, Z2, and Z3, Fig. 6). The first magnetic zone (Z1) is located in the northern and southern of the area and shows a low magnetic intensity, ranging from 42,840 nT to 42,853 nT. Meanwhile, the second magnetic zone (Z2) extends from western to central parts of the area and is characterized by its high magnetic intensity, varying from 42,859 nT to 42,864 nT. This zone may be related to manganese-iron ore deposits in Um-Bogma formation. The third magnetic zone (Z3) located at eastern part of the study area and characterized by its intermediate magnetic intensities, varying from 42,853 nT to 42,859 nT.

The total magnetic intensity map (Fig. 6) was reduced to the north magnetic pole (RTP), utilizing the known inclination and declination: $I = 42.6^\circ$, $D = 3^\circ$ of the study area. The RTP magnetic map (Fig. 7) displays nearly the same magnetic characters, which are illustrated on the total magnetic-intensity map (Fig. 6), with some stretching and repositioning of magnetic anomalies to the north.

5.2. Quantitative interpretation

Fast Fourier Transform (FFT), was applied on the TMI Data, using Oasis montaj program from Geosoft Inc. (*Geosoft, 2010*), to explore the frequency content of these data and select the suitable cut-off frequencies for both the high-pass (residual) and low-pass (regional) filtered maps. The inspection of the power spectrum curve (Fig. 8) distinguished the regional and residual magnetic components. The estimated average depths for the shallow-seated and deep-seated magnetic sources, as calculated from the power spectrum curve, reach 20 m and 75 m, respectively (Fig. 8).

5.3. Low-pass (regional) map

By examining the low-pass (regional) magnetic map (Fig. 9) of the deep magnetic sources, it was found that they take almost the same shape of the total magnetic intensity map (Fig. 6), but differently, the contour lines became wider and smoother. This could be due to the fact that most of the influence in the total magnetic map is due to deep sources.

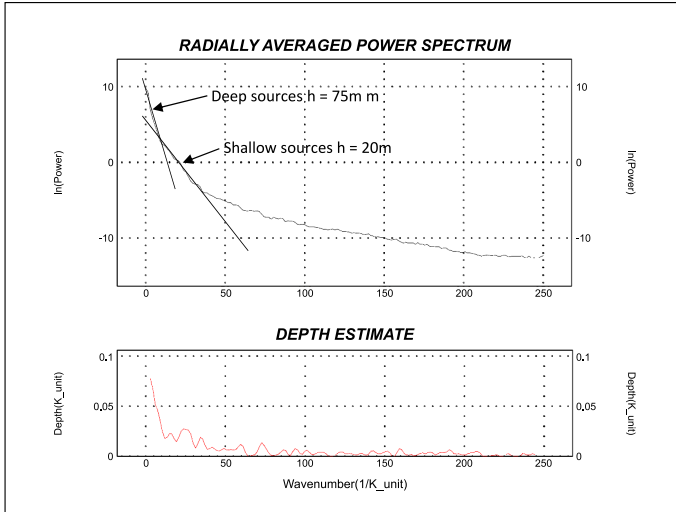


Fig. 8. Radially-averaged power spectrum and depth estimate of the total magnetic intensity data Al-Gor area, Southwestern Sinai, Egypt.

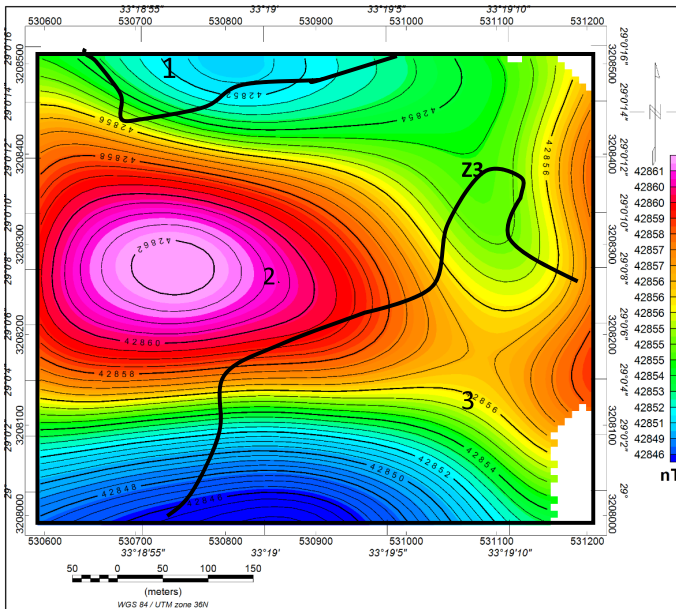


Fig. 9. Low-pass (regional) magnetic field map, at an average depth of 75m, Al-Gor area, Southwestern Sinai, Egypt.

5.4. High-pass (residual) map

The residual (high-pass) magnetic anomalies can be defined as the anomalies that are economically interesting, because they indicate shallow bodies (sources) and are characterized by weaker and more localized anomalies. The obtained high-pass (residual) map (Fig. 10) enhances the high frequency magnetic anomalies, which are related to shallow-seated sources (bodies) with varying geometries and locations. Visual inspection of this map shows successive elongated positive and negative anomalies of relatively moderate amplitudes and frequencies.

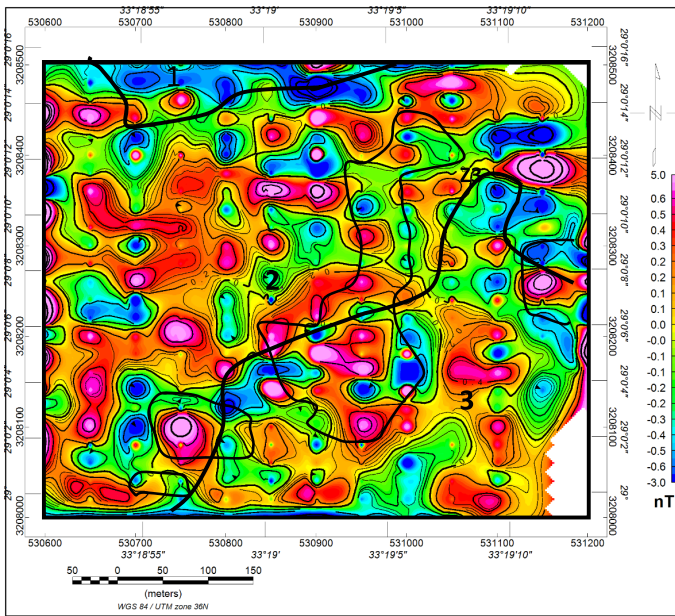


Fig. 10. High-pass (residual) magnetic field map, at an average depth of 20 m, Al-Gor area, Southwestern Sinai, Egypt.

6. Application of trend analysis on magnetic and radiometric data

Statistical analysis of the magnetic anomaly trend pattern is considered as a common quantitative approach to magnetic data interpretation. It was shown that magnetic trend patterns can be used to define magnetic

provinces which in turn reflect tectonic provinces.

One of the most useful geological applications of potential field surveys is to map surface structures as well as subsurface structural trends by following strike directions in magnetic and radiometric contours. Statistical analyses of these directions help in the delineation of the major tectonic trends that affected the deeply buried basement rocks as well as the overlying sedimentary cover, and consequently in deducing the directions of the tectonic stresses responsible for the creation of the associated geologic structures (*Affleck, 1963*).

The trend analysis techniques were performed on the filtered residual magnetic anomaly data as well as the total count radiometric anomaly data (Figs. 10 and 2) to define the prevailing structures trends that affected the studied area, and to check the relation which might exist among the inferred subsurface (magnetic) structural trends and the surface (radiometric) structural trends.

Close examination of the main interpreted structural trends as inferred from the surface as interpreted from the radiometric map and the subsurface as from residual magnetic map (Fig. 11) showed that the area under investigation was affected by three structural trends: two primary ones,

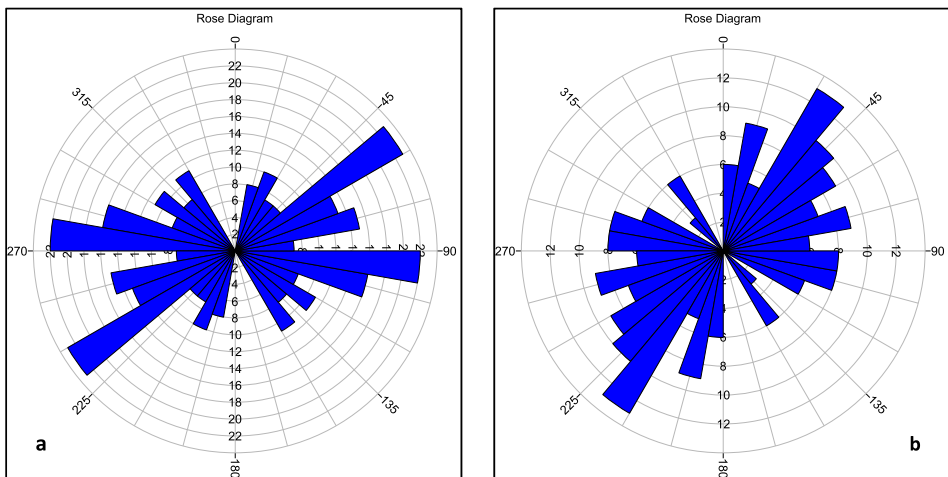


Fig. 11. Rose frequency diagrams showing the main interpreted magnetic structural lineaments (IMSL) as deduced from the high-pass (residual) map (a), and total-count map (b).

namely E–W and NE–SW, in addition to the NW–SE trend, a secondary direction. These fracturing trends are shown on the frequency diagrams (Fig. 11). This may indicate that the structures are continuous and extended from surface to subsurface and affects directly the accumulation the mineralization containing, high radioactive concentrations.

7. Conclusions

The gamma-ray spectrometric maps show different levels over the surveyed area, which reflect contrasting radioelement contents for the exposed various rock types. The study area possesses gamma radiations ranging between 0.6 and 110.9 Ur as a total count, 0.1 to 1.8% for K, 0.1 to 99 ppm for eU and 0.1 to 23 ppm for eTh.

Examination of spectrometric and ratio maps indicates a good agreement in the sites with high concentrations of uranium, deduced from the two methods of *Krasnov et al. (1980)* and *Broome (1990)* that used to determine the high concentrations of uranium, which gives great confidence in the results obtained, which may raise the probability to consider the study area as a new site for uranium exploration.

The studied rock types in study area gave from chemical analyses a greater amount of uranium than these radiometrically determined, reflecting a disequilibrium state characterised by addition of uranium.

The trends of the structures as derived from the spectrometric and ratio maps correspond to those inferred from the residual-component magnetic map, which reflects the effect of structures on the concentration of radioactive elements and, consequently mineralization.

From the application of spectral analyses of magnetic data, the regional and residual depths of magnetic anomalies were computed. The first depth represents the regional (deep) anomalies at about 75 m, and the residual (shallow) anomalies lies at about 20 m.

The area can be considered a promising area for the exploration of radioactive deposits as well as rare earth elements, which appeared well in chemical analyses. Therefore, it is recommended to conduct a survey of the area using electrical methods to trace the concentrations in depth, as most of the radioactive anomalies are related to the Um-Bogma formation, which contains iron and manganese in addition to gibbsite due to their properties.

Acknowledgements. The authors sincerely thank the reviewers and editors for their suggestions and comments, which have significantly improved the quality of this manuscript.

References

- Abdel-Azeem M. M., 2011: Geological, Mineralogical and Geochemical Studies of Soil Sediments, Al Gor Area, Southwestern Sinai, Egypt. Master Thesis, Faculty of Science, Helwan University, Egypt, 118 p.
- Affleck J., 1963: Magnetic anomaly trend and spacing patterns. *Geophysics*, **28**, 3, 379–395, doi: 10.1190/1.1439188.
- Alshami A. S., 2003: Structural and lithologic controls of uranium and copper mineralization in Um Bogma environs, South Western Sinai, Egypt. Ph.D. Thesis, Faculty of Science, Mansoura University, Egypt. 148 p.
- Alshami A. S., 2018: U-minerals and REE distribution, paragenesis and provenance, Um Bogma Formation southeastern Sinai, Egypt. *Nucl. Sci. Sci. J.*, **7**, 1, 31–55, doi: 10.21608/NSSJ.2018.30721.
- Alkhateeb S. A., Hossny A. A., Alshami A. S., Zaeimah M. A. M., 2019: Ground follow-up of the airborne gamma-ray spectrometric survey data, Ramlet Homayyer area, east Abu-Zeneima, southwestern Sinai, Egypt. *Appl. Radiat. Isot.*, **151**, 129–139, doi: 10.1016/j.apradiso.2019.05.036.
- Attia G. M., Mahdy A. I., Aly G. M., Abdel Gawad M. A., Abdel Azeem M. M., 2011: Mineralogical and geochemical characteristics of the Carboniferous paleosol, El Gor Area, South Western Sinai, Egypt. *Egypt. J. Geol.*, **55**, 397–417.
- Broome H. J., 1990: Generation and interpretation of geophysical images with examples from the Rae Province, northwestern Canada shield. *Geophysics*, **55**, 8, 977–997, doi: 10.1190/1.1442927.
- Durrance E. M., 1986: Radioactivity in Geology: Principles and Application. Ellis and Horwood, Chichester, 441 p.
- Geofyzika, 1997: Portable magnetometer, model PMG1, Instruction manual 1997, Brno, Czech Republic, 78 p.
- Geosoft, 2010: Geosoft mapping and processing system. Geosoft Inc., Toronto, Canada.
- IAEA (International Atomic Energy Agency), 1979: Gamma Ray Surveys in Uranium Exploration, Technical Reports Series No. 186, IAEA, Vienna.
- IAEA (International Atomic Energy Agency), 1988: Geochemical exploration for uranium. IAEA Technical Report Series No. 284, Vienna, Austria, 97 p.
- Krasnov A. I., Vysokoostrovskaya E. B., Smirnov V. A. et al., 1980: Geophysical airborne methods of uranium deposits prognostication. *Atomisdat*, Moscow, 1–128 (in Russian).
- Saunders D. F., Potts M. J., 1976: Interpretation and application of high sensitivity airborne gamma ray spectrometric data. In: IAEA Symp. Exploration for Uranium Ore Deposits, Vienna, 107–124.
- Soliman M. S., Abu El-Fetouh M. A., 1969: Petrology of Carboniferous sandstone in West Central Sinai. *J. Geol. U.A.R.*, **13**, 2, 61–143.